PHYSICAL REVIEW B **83**, 054410 (2011)

Spin relaxation in metallic ferromagnets

L. Berger
Physics Department, Carnegie Mellon University, Pittsburgh, Pennsylvania 15213, USA

(Received 14 October 2010; published 9 February 2011)

The Elliott theory of spin relaxation in metals and semiconductors is extended to metallic ferromagnets. Our treatment is based on the two-current model of Fert, Campbell, and Jaoul. The $d \rightarrow s$ electron-scattering process involved in spin relaxation is the inverse of the $s \rightarrow d$ process responsible for the anisotropic magnetoresistance (AMR). As a result, spin-relaxation rate $1/\tau_{\mathrm{sr}}$ and AMR $\Delta\rho$ are given by similar formulas, and are in a constant ratio if scattering is by solute atoms. Our treatment applies to nickel- and cobalt-based alloys which do not have spin-up $3d$ states at the Fermi level. This category includes many of the technologically important magnetic materials. And we show how to modify the theory to apply it to bcc iron-based alloys. We also treat the case of Permalloy $\mathrm{Ni}_{80}\mathrm{Fe}_{20}$ at finite temperature or in thin-film form, where several kinds of scatterers exist. Predicted values of $1/\tau_{\mathrm{sr}}$ and $\Delta\rho$ are plotted versus resistivity of the sample. These predictions are compared to values of $1/\tau_{\mathrm{sr}}$ and $\Delta\rho$ derived from ferromagnetic-resonance and AMR experiments in Permalloy.

DOI: 10.1103/PhysRevB.83.054410 PACS number(s): 76.60.Es, 76.50.+g, 72.15.Gd

I. INTRODUCTION

The accepted theory of spin relaxation in metals and semiconductors is due to Elliott.[1] Because of spin-orbit interaction, nominally spin-down states of the $3d$ band acquire a small spin-up admixture. Then, random electric potentials of phonons, solutes, or defects can induce spin-flip scattering events from down to up. A review paper by Yafet[2] summarizes early work on the theory. Experiments and theory in the case of phonon scattering have been connected successfully[3] for several monovalent and polyvalent nonmagnetic metals. Fulde and Luther, as well as Tserkovnyak *et al.* and Skadsem *et al.*,[4] have developed theories of spin relaxation specifically for ferromagnetic metals, as part of their work on Gilbert damping.

In metallic ferromagnets, the spin-relaxation rate $1/\tau_{\mathrm{sr}}$ is important because it influences the Gilbert damping parameter α associated with ferromagnetic-resonance linewidths. Inversely, the value of $1/\tau_{\mathrm{sr}}$ can be derived from the measured value of α, as we will see in Sec. V.

The purpose of the present paper is to develop a theory of spin relaxation in metallic ferromagnets. As in Refs. 4 and 5, the relaxation considered here is that of spin-down $3d$ electrons. This is different from the s-d exchange model, where only $4s$ conduction-electron spins are assumed to relax. Similarly, our theory does not apply to the phenomenon of giant magnetoresistance, where spin relaxation is important but the involved electrons are high-mobility $4s$ electrons. Nevertheless, since there are no spin-up $3d$ electrons at the Fermi level in the materials considered here (Sec. II), the final state of the relaxation process is a $4s\uparrow$ state (Fig. 1).

Our theory is based on the two-current model of electrical transport. In that model,[6–8] spin-up and spin-down charge carriers are assumed to each have unique and well-defined effective mass and momentum-relaxation rate, different from the other. Like spin relaxation,[1] the existence of the anisotropic magnetoresistance effect (AMR) depends[9] on spin-flip scattering processes. Both phenomena can be understood within the two-current model. We will make use of existing experimental data on AMR to determine the value of parameters of that model.

II. ELECTRONIC STATES AND SPIN RELAXATION

Band-structure calculations for Ni (Ref. 10) all show that the spin-up Fermi level is located above the top of the $3d$ band (Fig. 1), in a region with the low density of states and high electron velocity characteristic of $4s$ electrons. The spin-up Fermi surface of Ni even has[11] necks similar to those of Cu. This is confirmed by ordinary Hall-effect data[12] in fcc Ni-Cu, Ni-Fe-Cu, and Ni-Co, where the spin-up $3d$ band is also full. They show that a small number $\simeq 0.3$ electrons/at. of carriers carry the majority of the current. It is also confirmed by deviations from Matthiessen's rule[7,8] in the same kind of alloys, which indicate a large ratio 3-20 of spin-up to spin-down conductivities. Despite s-d hybridization, it is these distinct properties that justify giving the name $4s$ to these spin-up electrons at the Fermi level. The same properties make possible the existence of the giant magnetoresistance effect used in reading heads, the topic of the 2007 Nobel Prize in Physics, and the existence of the spin-transfer torque. Nickel-rich Ni-Fe, Ni-Zn, cobalt, Co-Ni, and cobalt-rich Co-Fe also belong to that class of materials, which fall on the right-hand side of the so-called Slater-Pauling curve of saturation magnetization versus electron concentration.

Alloys such as Ni-Cr, Ni-V, Ni-Mo, Ni-Mn, Co-Cr, and Co-Mn have[7,8] spin-up $3d$ states at the Fermi level. As explained at the end of Sec. III, our theory does not apply to them. With some modifications, it can cover the case of bcc iron alloys, as shown at that location.

The spin-down Fermi level of Ni or Co alloys is in the $3d$ band (Fig. 1). The Hamiltonian of itinerant $3d$ electrons is

$$\begin{aligned} H &= H_{\mathrm{kin}} + U(\mathbf{r}) + g\mu_B \mathbf{s}\mathbf{H}_{\mathrm{ex}} + H_{\mathrm{so}} + V(\mathbf{r}), \\ H_{\mathrm{so}} &= \xi\left[\tfrac{1}{2}(L_+ s_- + L_- s_+) + L_z s_z\right], \\ V(\mathbf{r}) &= \Sigma_{i=1}^{N_{\mathrm{sc}}} v(\mathbf{r} - \mathbf{r_i}). \end{aligned} \tag{1}$$

Here, H_{kin} is the kinetic energy, $U(\mathbf{r})$ is the crystal periodic potential energy, $\mathbf{H}_{\mathrm{ex}}$ is the Stoner d-d exchange field, and H_{so} is the spin-orbit energy associated with $U(\mathbf{r})$. Also, $V(\mathbf{r})$ is the total potential energy of scatterers, $v(\mathbf{r} - \mathbf{r_i})$ is the energy of a single scatterer at location $\mathbf{r_i}$, and N_{sc} the total number of

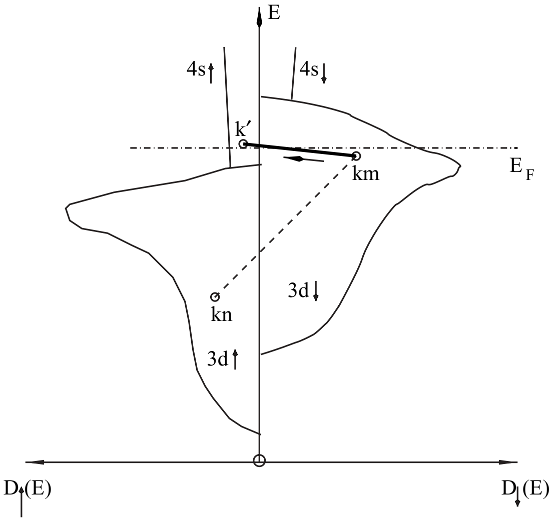

FIG. 1. Band structure of fcc Ni and Ni alloys. The spin-up and spin-down densities of states $D_\uparrow$ and $D_\downarrow$ are plotted vs energy E. A $d \rightarrow s$ spin-relaxation process [Eq. (3)] is shown as a thick solid near-horizontal line. It goes from a spin-down $3d$ state, labeled $\mathbf{k}$ and m, to a spin-up $4s$ state labeled $\mathbf{k}'$. Spin-up admixtures [Eq. (2)], labeled $\mathbf{k}$ and n, to a spin-down $3d$ state labeled $\mathbf{k}$ and m, are indicated by an oblique dashed line.

scatterers. The $+z$ axis is parallel to the total $3d$ spin. In a pure metal, the spin-down eigenstates of $H_{\text{kin}} + U + g\mu_B \mathbf{s}\mathbf{H}_{\text{ex}}$ are Bloch waves $\chi_-(s_z)\phi_{km}(\mathbf{r})$, where $m = 1$–5 is a band index. As shown by Hodges *et al.*[13] and discussed by Herring,[14] there are $4s$ admixtures to states of the $3d$ band, but these admixtures have only a minor effect on the width and structure of that band. For simplicity, they will be ignored here.

If, in addition, we switch H_{so} on, the nominally spin-down eigenstates near the Fermi level, labeled by indices $\mathbf{k}$ and $m = 1$–5 (Fig. 1), become[1]

$$\psi^\downarrow_{km} \simeq \chi_-(s_z)\phi_{km} + \Sigma_n b_{kmn}\chi_+(s_z)\phi_{kn}, \qquad (2)$$

where the small dimensionless coefficients b_{kmn} are given by first-order perturbation theory. These spin-up admixtures to spin-down states are labeled by indices $\mathbf{k}$ and $n = 1$–5 (Fig. 1), and are caused by the spin-flip part $L_+s_- + L_-s_+$ of H_{so}. Since H_{so} originates from the periodic potential $U(\mathbf{r})$, it is itself a periodic operator. Therefore, $\mathbf{k}$ commutes with H_{so}, and only states of the same $\mathbf{k}$ and different n are mixed together by H_{so}. The nonflip part $L_z s_z$, only affecting the g factor, will be ignored.

We consider a spin-relaxation process where the total $3d$ spin increases toward its equilibrium value, through one-electron processes. As will be explained in Sec. V in relation to Gilbert damping, usually only the spin relaxation of states near the Fermi level matters. Therefore, the important scattering event, shown as a thick nearly horizontal solid line in Fig. 1, is from the $3d \downarrow$ state $\psi^\downarrow_{km}$ to a $4s \uparrow$ state $\chi_+(s_z)\phi^{4s}_{k'}$. Using the first Born approximation, we have

$$1/\tau_{\text{sr}} = \frac{2\pi}{\hbar}\overline{\left|\left\langle\psi^\downarrow_{km}\middle|V(\mathbf{r})\chi_+(s_z)\phi^{4s}_{k'}\right\rangle\right|^2} D_\uparrow(E_F). \qquad (3)$$

The horizontal bar indicates an average over $\mathbf{k}$ and $\mathbf{k}'$ at the Fermi level E_F, and $D_\uparrow(E)$ is the $4s \uparrow$ density of states. We have ignored increases of the magnitude of the spin-down $3d$ wave function at the location of scatterers caused by $3d$ scattering resonances. We also ignore the effect of H_{so} on the $4s \uparrow$ states. We combine Eqs. (2) and (3). In the square of the matrix element in Eq. (3), the double products coming from the index i disappear because scatterers are at random locations. Then

$$\begin{aligned} 1/\tau_{\text{sr}} &= \frac{2\pi}{\hbar}\overline{|\Sigma_n b^*_{kmn} J^+_{kk'n}|^2} N_{\text{sc}} D_\uparrow(E_F), \\ J^+_{kk'n} &= \left\langle \phi_{kn}\middle|v(\mathbf{r})\phi^{4s}_{k'}\right\rangle. \end{aligned} \qquad (4)$$

We see that spin relaxation is made possible[1] by the spin-up admixtures to spin-down $3d$ states, represented by coefficients b_{kmn} in Eq. (4).

III. ELECTRICAL CONDUCTION AND AMR

The spin-up and spin-down momentum-relaxation times $\tau_\uparrow, \tau_\downarrow$ are related to the corresponding zero-field resistivities $\rho_\uparrow$, $\rho_\downarrow$:

$$\rho_\uparrow = \frac{m_\uparrow}{e^2 n_\uparrow \tau_\uparrow}, \quad \rho_\downarrow = \frac{m_\downarrow}{e^2 n_\downarrow \tau_\downarrow}. \qquad (5)$$

Here, $m_\uparrow, m_\downarrow$ and $n_\uparrow, n_\downarrow$ are the spin-up and spin-down effective masses and electron densities. The measured zero-field resistivity ρ is given by

$$\rho^{-1} = \rho_\uparrow^{-1} + \rho_\downarrow^{-1}. \qquad (6)$$

The value of $\tau_\uparrow$ is limited by $s \rightarrow s$ scattering processes, represented by a relaxation time $\tau^{ss}_\uparrow$. Because of the spin-up admixtures to spin-down $3d$ states, already mentioned, $s \rightarrow d$ scattering from $4s \uparrow$ states is also possible.[7] Using Eq. (2) and the same ideas as mentioned earlier, we obtain

$$1/\tau_\uparrow = \frac{2\pi}{\hbar}\overline{|\Sigma_n b^*_{kmn} J^+_{kk'n}|^2} N_{\text{sc}} D_\downarrow(E_F) + 1/\tau^{ss}_\uparrow. \qquad (7)$$

Here, $D_\downarrow(E)$ is the spin-down density of states. The first term of Eq. (7) is very similar to Eq. (4), because the $s \rightarrow d$ scattering processes involved in $1/\tau_\uparrow$ are exactly the inverse (Fig. 1) of the $d \rightarrow s$ processes responsible for $1/\tau_{\text{sr}}$.

As stated earlier, the spin-down states $\chi_-(s_z)\phi_{km}$ at the Fermi level are mostly $3d$ in character, with a high density of states. Therefore, we can neglect $s \rightarrow s$ scattering and spin-orbit interaction when calculating $1/\tau_\downarrow$ to use in Eq. (5). Nevertheless, one sheet of the spin-down Fermi surface, called *s-d* (Ref. 10) and with states $\chi_-(s_z)\phi^{sd}_k$, has a smaller effective mass $m_\downarrow$ than others and may carry most of the spin-down current. This is confirmed by data of cyclotron resonance for Ni, discussed in Sec. V, which show $m_\downarrow$ smaller than $m_\uparrow$. Then we write

$$\begin{aligned} 1/\tau_\downarrow &= \frac{2\pi}{\hbar}\overline{|J^-_{kk'm}|^2} N_{\text{sc}} D_\downarrow(E_F), \\ J^-_{kk'm} &= \left\langle \phi_{km}\middle|v(\mathbf{r})\phi^{sd}_{k'}\right\rangle. \end{aligned} \qquad (8)$$

In experiments of AMR, the resistivities $\rho^\parallel, \rho^\perp$ are measured in the magnetically saturated state, with current parallel and perpendicular to the magnetization, respectively. The AMR is $\Delta\rho = \rho^\parallel - \rho^\perp$. Similarly, we define spin-up and spin-down resistivities $\rho_\uparrow^{\|}, \rho_\downarrow^{\|}, \rho_\uparrow^{\perp}, \rho_\downarrow^{\perp}$ in the saturated state. They obey the following relations:

$$(\rho^{\|})^{-1} = (\rho_\uparrow^{\|})^{-1} + (\rho_\downarrow^{\|})^{-1}, \quad (\rho^{\perp})^{-1} = (\rho_\uparrow^{\perp})^{-1} + (\rho_\downarrow^{\perp})^{-1}. \tag{9}$$

Then, we can define the spin-up and spin-down anisotropies $\Delta\rho_\uparrow = \rho_\uparrow^{\|} - \rho_\uparrow^{\perp}$ and $\Delta\rho_\downarrow = \rho_\downarrow^{\|} - \rho_\downarrow^{\perp}$.

We use Eqs. (6) and (9) to derive the Dorleijn-Miedema relation[15] between the various anisotropies:

$$\Delta\rho = \Delta\rho_\uparrow \left(\frac{\rho}{\rho_\uparrow}\right)^2 + \Delta\rho_\downarrow \left(\frac{\rho}{\rho_\downarrow}\right)^2. \tag{10}$$

Campbell, Fert, and Jaoul[7] have derived the relation $\Delta\rho_\uparrow = -\Delta\rho_\downarrow$ from the normalization condition for the $3d$ wave function. However, Eq. (10) shows that the choice of $\Delta\rho_\downarrow$ has little effect on the value of $\Delta\rho$, in the nickel alloys considered here where $\rho_\downarrow \ll \rho_\uparrow$. Instead, we simply assume $\Delta\rho_\downarrow = 0$. Then, Eqs. (10) and (6) give

$$\Delta\rho = \frac{\Delta\rho_\uparrow}{(1 + \rho_\uparrow/\rho\downarrow)^2}. \tag{11}$$

In the AMR theory of Smit,[9] $\Delta\rho_\uparrow$ is caused by a corresponding anisotropy $\Delta(1/\tau_\uparrow)$ of $1/\tau_\uparrow$. Writing in the saturated state equations similar to Eqs. (5), for current parallel and perpendicular to the magnetization, we obtain

$$\Delta\rho_\uparrow = \frac{m_\uparrow}{n_\uparrow e^2}\Delta(1/\tau_\uparrow). \tag{12}$$

Also writing Eq. (7) for current parallel and perpendicular, we have

$$\Delta(1/\tau_\uparrow) = \frac{2\pi}{\hbar} N_{\mathrm{sc}} D_\downarrow(E_F) \Delta(\overline{|\Sigma_n b_{kmn}^* J_{kk'n}^+|^2}). \tag{13}$$

While the details of the process of averaging over $\mathbf{k}$ and $\mathbf{k}'$ in Eqs. (3), (4), (7), and (8) were not critical, in the case of Eq. (13) the contribution of each $\mathbf{k}'$ must have a weight proportional to the square of the cosine of the angle between $\mathbf{k}'$ and the current. Finally, we combine Eqs. (5)–(8) and (11)–(13),

$$\rho\uparrow = \delta\rho_\downarrow + \rho_\uparrow^{ss}, \quad \rho_\uparrow^{ss} = \frac{m_\uparrow}{n_\uparrow e^2 \tau_\uparrow^{ss}}, \tag{14}$$

$$\begin{gathered} \Delta\rho = \frac{\gamma\rho_\downarrow}{(1 + \rho_\uparrow/\rho\downarrow)^2}, \quad \delta = \frac{m_\uparrow/n_\uparrow}{m_\downarrow/n_\downarrow}\frac{\overline{|\Sigma_n b_{kmn}^* J_{kk'n}^+|^2}}{\overline{|J_{kk'm}^-|^2}}, \\ \gamma = \frac{m_\uparrow/n_\uparrow}{m_\downarrow/n_\downarrow}\frac{\Delta(\overline{|\Sigma_n b_{kmn}^* J_{kk'n}^+|^2})}{\overline{|J_{kk'm}^-|^2}}. \end{gathered} \tag{15}$$

Note that the quantities δ and γ are independent of the number N_{sc} of scatterers. For solute scatterers, if the range of $v(\mathbf{r})$ is the electrostatic shielding length of the Ni matrix, they will also be independent of the nature of the solutes. Campbell, Fert, and Jaoul[8] have shown experimentally that γ has a value 0.01 for solute scattering in Ni dilute alloys at low temperature.

Campbell, Fert, and Pomeroy[6,7] have introduced a coupling between spin-up and spin-down electron gases, through collisions with thermal magnons. We will ignore this "spin mixing" for two reasons. First, such inelastic collisions should cause a reduction of the Lorenz number. But heat-transport data show no such reduction.[16] Also, measured $\Delta\rho$ values versus temperature[17] in alloys are nearly equal to values versus thin-film thickness[18] for given resistivity. This fact cannot be explained on the basis of spin mixing, and suggests that spin mixing is not needed.

Similarly, by combining Eqs. (4), (5), and (8), we obtain

$$1/\tau_{\mathrm{sr}} = \delta\frac{D_\uparrow(E_F)}{D_\downarrow(E_F)}\frac{n_\uparrow e^2}{m_\uparrow}\rho_\downarrow. \tag{16}$$

This equation is the main result of the present paper. In the Elliott theory[1] of spin relaxation in nonmagnetic materials, it was found that $1/\tau_{\mathrm{sr}}$ was proportional to the electrical resistivity ρ. In the case of a metallic ferromagnet, our Eq. (16) shows that $1/\tau_{\mathrm{sr}}$ is proportional to $\rho_\downarrow$. Note that the latter is larger than $\rho_\uparrow$ or the measured resistivity ρ, by a factor that depends on the nature of scatterers and reaches 20 in bulk Ni-Fe and Ni-Co at low temperature.

Equations (15) and (16) predict that $1/\tau_{\mathrm{sr}}$ and $\Delta\rho$ remain in a constant ratio as $\rho_\downarrow$ or the nature of solutes changes, if we neglect the variation of the factor $(1 + \rho_\uparrow/\rho_\downarrow)^2$; usually, that factor is only slightly larger than 1, since $\rho_\uparrow \ll \rho_\downarrow$. This prediction applies to various dilute solutes such as Cu, Co or Fe in a Ni matrix, or Ni or Fe in a Co matrix; these solutes are chosen to keep the spin-up $3d$ band full. Note that the prediction holds only for solute scattering at low temperature (see Secs. V and VI).

The presence[7,8] of spin-up $3d$ states at the Fermi level of Ni-Cr, Ni-V, Ni-Mn, Co-Cr, and Co-Mn causes changes in the value of the quantity $D_\uparrow n_\uparrow/(D_\downarrow m_\uparrow)$ appearing in Eq. (16). These changes depend on the nature of the solute. Therefore, the earlier prediction of $1/\tau_{\mathrm{sr}}$ and $\Delta\rho$ being in a constant ratio does not apply to this class of alloys. But, since these alloys fall below the Slater-Pauling curve, their saturation magnetization is usually small, and they are not very important as magnetic materials.

In bcc iron alloys such as Fe-Cr, Fe-V, and iron-rich Fe-Co, the spin-down Fermi level is pinned in a gap of the $3d$ band. As a result,[6] we have $D_\uparrow \gg D_\downarrow$ and $\rho_\downarrow \gg \rho_\uparrow$. Therefore, the roles of the spin-up and spin-down $3d$ bands are interchanged. The present theory is still valid provided $\rho_\uparrow$ is replaced by $\rho_\downarrow$ everywhere and vice versa. For example, $1/\tau_{\mathrm{sr}}$ and $\Delta\rho$ are still in a constant ratio for solute scattering. These iron alloys are on the left-hand side of the Slater-Pauling curve.

IV. PREDICTED $\Delta\rho$ FOR PERMALLOY WITH TWO KINDS OF SCATTERERS

In the Ni or Co alloys considered here, solute scattering[7,8] gives much larger value of $\Delta\rho/\rho$ than phonon,[16] surface, or grain-boundary[19] scattering. Therefore, we will lump together the spin-up $s \rightarrow s$ resistivities generated by the various scatterers of the second class into a quantity $\rho_{\uparrow g}^{ss}$. The corresponding quantity for solute scattering is $\rho_{\uparrow \mathrm{sol}}^{ss}$. We write Matthiessen's rule for spin-up $s \rightarrow s$ scattering as

$$\rho_\uparrow^{ss} = \rho_{\uparrow \mathrm{sol}}^{ss} + \rho_{\uparrow g}^{ss}. \tag{17}$$

For $\rho_\downarrow$, we also use Matthiessen's rule and write a sum of two terms. Because of $s \rightarrow d$ scattering in the spin-down band, with $D_\downarrow \gg D_\uparrow$, each term is a multiple $\alpha_{\mathrm{sol}} > 1$ or $\alpha_g > 1$ of the corresponding term of $\rho_\uparrow^{ss}$,

$$\rho_\downarrow = \alpha_{\mathrm{sol}}\rho_{\uparrow\mathrm{sol}}^{ss} + \alpha_g\rho_{\uparrow g}^{ss}. \tag{18}$$

Then, we substitute Eqs. (17) and (18) into the first Eq. (14),

$$\rho_\uparrow = (\delta\alpha_{\mathrm{sol}} + 1)\rho_{\uparrow\mathrm{sol}}^{ss} + (\delta\alpha_g + 1)\rho_{\uparrow g}^{ss}. \tag{19}$$

We treat the case of Permalloy, that is, of $\mathrm{Ni}_{100-x}\mathrm{Fe}_x$, with $x = 15$–25 at. %. We start with bulk Permalloy at low temperature, where $\rho_{\uparrow g}^{ss} \simeq 0$. The need to fit measured values of ρ and $\Delta\rho$ in the bulk at low temperature constrains the choice of $\rho_{\uparrow\mathrm{sol}}^{ss}$ and α_{sol} in Eqs. (18), (19), and (15). We choose $\rho_{\uparrow\mathrm{sol}}^{ss} = 0.8 \times 10^{-8}\ \Omega\,\mathrm{m}$ and $\alpha_{\mathrm{sol}} = 100$. We use the same $\gamma = 0.01$ as mentioned earlier for dilute Ni alloys. Then, the correction factor $(1 + \rho_\uparrow/\rho_\downarrow)^2$ takes the value 1.126. And Eqs. (18), (19), (15), and (6) yield $\rho = 3.81 \times 10^{-8}\ \Omega\,\mathrm{m}$ and $\Delta\rho = 0.726 \times 10^{-8}\ \Omega\,\mathrm{m}$. These give the extreme left-hand point of the solid curves in Fig. 2, and are in fair agreement with corresponding experimental data for bulk Permalloy at 4 or 20 K, also on the left-hand side of Fig. 2.

As we increase T or go to thin films, thus introducing phonons, grain boundaries, or surfaces, $\rho_{\uparrow g}^{ss}$ increases from zero. The correction factor increases, too. The predicted values of ρ and $\Delta\rho$, given by Eqs. (18), (19), (15), and (6), are plotted as solid lines in Fig. 2, for α_g equal to 2 and 4. Bozorth,[20] Van Elst,[17] Berger and Rivier,[21] and McGuire and Potter[22] have measured ρ and $\Delta\rho$ of bulk Permalloy at various temperatures. Mitchell[18] and Williams and Mitchell[23] have done similar measurements on Permalloy films of variable thickness, at room temperature. These data sets are shown as various symbols in Fig. 2. The differences between them are partly caused by slight Fe concentration differences. We see that $\alpha_g = 2$ gives a better agreement, at high values of ρ, between predicted and measured values of $\Delta\rho$ in thin films than $\alpha_g = 4$.

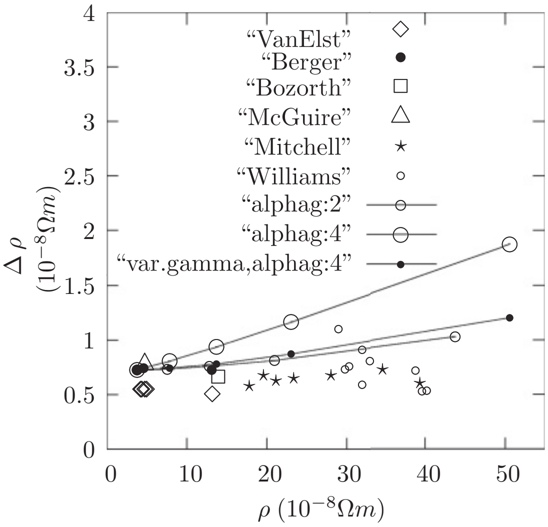

FIG. 2. Anisotropic magnetoresistance $\Delta\rho$ vs resistivity ρ for Permalloy. The solid curves labeled "alphag:2" and "alphag:4" are predictions for constant $\gamma = 0.01$, with $\alpha_g = 2$ and 4, respectively (Sec. IV). The solid curve labeled "var.gamma,alphag:4" is the prediction of the variable-γ theory of Sec. VI with $\gamma_g = 0.005, \gamma_{\mathrm{sol}} = 0.01$, and $\alpha_g = 4$. The data points represent measured $\Delta\rho$ values for bulk samples with variable temperature, and for thin films with variable thickness.

V. PREDICTED $1/\tau_{\mathrm{sr}}$ FOR PERMALLOY WITH TWO KINDS OF SCATTERERS

Again, we consider Permalloy. The ratio $D_\uparrow(E_F)/D_\downarrow(E_F)$ in Eq. (16) is the same as the ratio of spin-up and spin-down electronic specific-heat coefficients $\gamma_\uparrow^{\mathrm{el}}/\gamma_\downarrow^{\mathrm{el}}$. Since $\gamma_\uparrow^{\mathrm{el}} \ll \gamma_\downarrow^{\mathrm{el}}$, we have[24] $\gamma_\downarrow^{\mathrm{el}} \simeq \gamma^{\mathrm{el}} = 4.2\,\mathrm{mJ/mol\,K^2}$. Since $\gamma_\uparrow^{\mathrm{el}}$ is not directly measurable in Permalloy, we start with the experimental value $\gamma_\uparrow^{\mathrm{el}} = \gamma^{\mathrm{el}}/2 = 0.347\ \ \mathrm{mJ/mol\,K^2}$ for Cu.[25] Band-structure calculations indicate that $D_\uparrow(E_F)$ is larger in Ni (Ref. 10) than in Cu,[26] by a factor 1.44. Applying this correction factor to the Cu value, we obtain $\gamma_\uparrow^{\mathrm{el}} = 0.500\ \mathrm{mJ/mol\,K^2}$ for Ni or Permalloy. Thus, finally, $D_\uparrow(E_F)/D_\downarrow(E_F) = \gamma_\uparrow^{\mathrm{el}}/\gamma_\downarrow^{\mathrm{el}} = 0.119$. This procedure allows us to take into account electron-phonon enhancement effects.

Ordinary Hall-effect measurements[12] in Ni-rich Ni-Cu, Ni-Fe-Cu, and Ni-Co show that fewer than 0.3 electrons per atom carry most of the current, at low temperature. We will use a value 0.275 electrons/at., corresponding to $n_\uparrow = 2.51 \times 10^{28}$ electrons/m^3. Cyclotron-resonance[27] data give $m_\uparrow = 46.4 \times 10^{-31}$ kg for the spin-up electron effective mass in Ni, over the belly of the Fermi surface away from its necks. We will also use this for $m_\uparrow$ in Permalloy. By its definition [Eq. (14)], δ must be somewhat larger than $\gamma = 0.01$. Therefore, we choose $\delta = 0.141$.

We calculate $\rho_\downarrow$ versus $\rho_{\uparrow g}^{ss}$ by Eq. (18), as in the last section. Then, Eq. (16) gives $1/\tau_{\mathrm{sr}}$. Also, we find ρ by Eqs. (18), (19), and (6), as done earlier. The $1/\tau_{\mathrm{sr}}$ values are plotted versus ρ in Fig. 3 as solid lines for the same parameters as before, $\alpha_{\mathrm{sol}} = 100$ and α_g equal to 2 and 4.

Now, we compare these predicted $1/\tau_{\mathrm{sr}}$ to those derived from the measured Gilbert constant α. There are two different

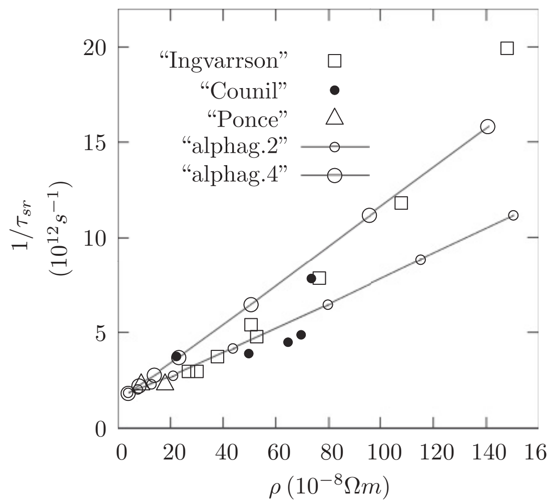

FIG. 3. Spin-relaxation rate $1/\tau_{\mathrm{sr}}$ vs resistivity ρ for Permalloy. The solid curves labeled "alphag.2" and "alphag.4" are predictions by the theory of Secs. IV and V with two kinds of scatterers, for $\alpha_g = 2$ and 4, respectively. The data points represent values of $1/\tau_{\mathrm{sr}}$ derived from measurements of the Gilbert damping constant for thin-film samples with variable temperature and with variable thickness.

kinds of electron mechanisms for Gilbert damping.[28] In one of them,[29] α decreases with increasing ρ. In the other,[4,5,30] it increases with increasing ρ. Measurements of α in Permalloy films of variable thickness by Ingvarsson *et al.*[31] and by Counil *et al.*[32] show that the second kind of mechanism is dominant in this material, except possibly at the lowest ρ values. As mentioned in the introduction, we are interested in the spin relaxation of $3d$ electrons. Therefore, we interpret the α data with the so-called d-d model,[4,5] not with the s-d exchange model.[30] The latter is more complex and, illogically, attributes spin relaxation to $4s$ electrons only. The d-d model yields[4,5]

$$\alpha = \frac{1}{\omega_d \tau_{\mathrm{sr}}}, \tag{20}$$

where $\omega_d = J_{dd} S/\hbar$ is the precession frequency of itinerant $3d$electrons in the Stoner exchange field, $J_{dd} = 0.5$ eV is the d-d exchange integral, and $S \simeq 0.47$ is the average atomic spin in Permalloy. Our unpublished quantum-mechanical derivation of Eq. (20) from the d-d model indicates that the net electron-spin relaxation rate $1/\tau_{\mathrm{sr}}$ vanishes except for states near the Fermi level. This is a consequence of the Pauli exclusion principle, and manifests itself by factors df/dE in the expression for the $1/\tau_{\mathrm{sr}}$ appearing in Eq. (20). Here, f is the Fermi-Dirac occupation number of an electron state of energy E. Such factors vanish away from the Fermi level. The same factors appear, for the same reasons, in quantum treatments[30] of Gilbert damping based on the s-d exchange model.

Ponce, Bhagat, and Lubitz[33] measured α on a Permalloy film of thickness 270.7 nm, between 4 and 300 K. The parameter G that they used is related to α by $G = \gamma M_s \alpha$, where $\gamma = (g/2) \times 1.76 \times 10^7$ rad/s Oe, $g = 2.10$, and $M_s \simeq 800$ emu/cm^3. Although they did not measure ρ, it can be roughly estimated from existing data for similar bulk and thin-film samples. Values of $1/\tau_{\mathrm{sr}}$ are obtained from these α values by solving Eq. (20). The α and ρ data by Ingvarsson *et al.*[31] and by Counil *et al.*[32] for Permalloy films of variable thickness are also used to obtain $1/\tau_{\mathrm{sr}}$ versus ρ. These "experimental" values of $1/\tau_{\mathrm{sr}}$ are shown as various kinds of data points in Fig. 3.

Over the whole range of ρ (Fig. 3), the best overall agreement between the Ingvarsson data and two-scatterer theory [Eqs. (16) and (18)] is obtained for $\alpha_{\mathrm{sol}} = 100$ and $\alpha_g = 4$. The data show more curvature than the theory. We give less importance to the Counil data (Fig. 3), because they extend over a much smaller range of ρ; but, because of their fast increasing slope (Fig. 3), they would probably yield an α_g value even larger than 4 if they were extended to higher ρ values.

This differs from the conclusion of the preceding section, where $\alpha_g = 2$ gave the best fit between theory and data for $\Delta\rho$. The next section will show how this contradiction can be resolved.

VI. VARIABLE-γ THEORY

In his theory of AMR,[9] Smit already suggested that phonon or defect scattering would be intrinsically less anisotropic than solute scattering. In other words, the quantity γ of Eq. (15) may depend on the nature of the scatterer. But this idea was ignored by Campbell, Fert, and Pomeroy,[6,7] who introduced spin mixing instead. If various scatterers contribute additively to $\Delta\rho$, a variable γ will have the following form:

$$\gamma = \frac{\gamma_{\mathrm{sol}}\alpha_{\mathrm{sol}}\rho^{ss}_{\uparrow\mathrm{sol}} + \gamma_g \alpha_g \rho^{ss}_{\uparrow g}}{\alpha_{\mathrm{sol}}\rho^{ss}_{\uparrow\mathrm{sol}} + \alpha_g \rho^{ss}_{\uparrow g}}, \tag{21}$$

where γ_{sol} and γ_g are two constants. We already know[8] that $\gamma_{\mathrm{sol}} \simeq 0.01$ in dilute Ni alloys. Unpublished calculations with a simple Einstein model of lattice vibrations yield $\gamma_g \simeq 0.7\gamma_{\mathrm{sol}} \simeq 0.007$.

By combining Eqs. (15), (21), and (18), we have $\Delta\rho = (\gamma_{\mathrm{sol}}\alpha_{\mathrm{sol}}\rho^{ss}_{\uparrow\mathrm{sol}} + \gamma_g\alpha_g\rho^{ss}_{\uparrow g})/(1 + \rho_\uparrow/\rho_\downarrow)^2$. Except for the slow-varying correction factor $(1 + \rho_\uparrow/\rho_\downarrow)^2$, this shows that the rate of variation of $\Delta\rho$ depends only on the product $\gamma_g\alpha_g$. Indeed, Fig. 2 shows that a variable γ with $\alpha_g = 4, \gamma_g = 0.005, \gamma_{\mathrm{sol}} = 0.01$ gives almost the same $\Delta\rho$ curve as the constant γ of Sec. IV with $\alpha_g = 2, \gamma_g = 0.01 = \gamma_{\mathrm{sol}}$. Of course, the value of γ_g has no effect on $1/\tau_{\mathrm{sr}}$.

Thus, the use of a variable γ [Eq. (21)] removes the contradiction encountered in Sec. V, allowing us to fit both $\Delta\rho$ and $1/\tau_{\mathrm{sr}}$ data with the same value $\alpha_g = 4$ (Figs. 2 and 3).

Hall-effect experiments show[12] an increase of $n_\uparrow$ when solute scattering is replaced by phonon scattering in Ni-Cu, Ni-Fe-Cu, and Ni-Co alloys. In turn, this causes an increase of $1/\tau_{\mathrm{sr}}$ in Eq. (16). This might provide an alternate explanation for the discrepancies between $\Delta\rho$ and $1/\tau_{\mathrm{sr}}$ discussed here, provided this $n_\uparrow$ increase also exists for surface and grain-boundary scattering. Finally, the saturation magnetization M_s and other magnetic properties of very thin Permalloy films of the highest resistivity (Fig. 3) have been found[34] to deviate from their normal values. This may give still another explanation. The severity of this effect is probably less with modern deposition techniques.

VII. EFFECT OF SPIN-ORBIT INTERACTION GENERATED BY THE SCATTERING POTENTIAL $V(\mathbf{r})$

So far, we used the spin-orbit interaction H_{so} associated with the periodic potential $U(\mathbf{r})$ [Eqs. (1)]. But the random potential $V(\mathbf{r})$ generates[2] a different kind of spin-orbit interaction, which we call H^V_{so}. The spin-relaxation rates caused by the two interactions are of the same order of magnitude. Like H_{so}, H^V_{so} causes an AMR $\Delta\rho$, ignored by Smit[9] and Fert,[6–8] which is also proportional to $\rho_\downarrow$ [Eq. (15)], and is also in a nearly fixed ratio to the corresponding $1/\tau_{\mathrm{sr}}$. Although the value of that ratio is not quite the same as before, the main conclusions of the present paper are not changed.

VIII. CONCLUSIONS

The two-current model, used by Campbell, Fert, and Jaoul[6–8] for their AMR theory, is also useful to understand spin relaxation. Both AMR and spin relaxation are based on the spin-flip part of spin-orbit interaction [Eqs. (1)]. AMR $\Delta\rho$ and relaxation rate $1/\tau_{\mathrm{sr}}$ are predicted to be in a constant ratio as the concentration or nature of solute scatterers is changed [Eqs. (15) and (16)]. Our theory covers nickel- and cobalt-based alloys which do not have spin-up $3d$ states at the Fermi level. This category includes many of the important magnetic materials. With appropriate modifications, our treatment also applies to bcc iron-based alloys. We treat in detail the case of Permalloy at $T > 0$ or in thin-film form, where two different kinds of scatterers exist. Parameters of the two-current model are partly determined from existing AMR data (Sec. IV and Fig. 2). The spin-relaxation rate $1/\tau_{\text{sr}}$ is predicted to increase linearly with increasing resistivity as temperature or film thickness is varied (Sec. V and Fig. 3). This prediction is compatible with spin-relaxation rates derived from FMR linewidth experiments in Permalloy (Fig. 3).

Our theory of spin relaxation in ferromagnetic metals differs in several respects from those of Fulde and Luther and of Tserkovnyak *et al.*[4] mentioned in the introduction. First, we recognize the fact that the spin-up Fermi level is located outside the $3d$ band (Fig. 1) in many important materials. Also, we take into account the degeneracy of the $3d$ band explicitly (Sec. II) through the index $n = 1$–5. Finally, we use the two-current model[6–8] (Sec. IV), in which the spin-up and spin-down resistivities are different by a factor that can reach 20 in Ni-Fe and Ni-Co.

As was explained before Eq. (20), the d-d model[4,5] is simpler and more logical than the s-d exchange model to treat Gilbert damping. Nevertheless, the s-d exchange model may well[35] be more reasonable and realistic for the problem of current-induced torques on domain walls. This comes[35] from the dominant role of high-mobility $4s\uparrow$ electrons in electrical transport.

---

[1] R. J. Elliott, Phys. Rev. **96**, 266 (1954).

[2] Y. Yafet, in *Solid State Physics*, edited by F. Seitz and D. Turnbull (Academic, New York, 1963), Vol. 14, p. 67.

[3] F. Beuneu and P. Monod, Phys. Rev. B **18**, 2422 (1978); P. Monod and F. Beuneu, *ibid.* **19**, 911 (1979); J. Fabian and S. Das Sarma, Phys. Rev. Lett. **81**, 5624 (1998); **83**, 1211 (1999).

[4] Y. Tserkovnyak, H. J. Skadsem, A. Brataas, and G. E. W. Bauer, Phys. Rev. B **74**, 144405 (2006); H. J. Skadsem, Y. Tserkovnyak, A. Brataas, and G. E. W. Bauer, *ibid.* **75**, 094416 (2007); P. Fulde and A. Luther, Phys. Rev. **175**, 337 (1968).

[5] L. Berger, Phys. Rev. B **80**, 144427 (2009).

[6] I. A. Campbell, A. Fert, and A. R. Pomeroy, Philos. Mag. **15**, 977 (1967); A. Fert and I. A. Campbell, J. Phys. F **6**, 849 (1976).

[7] I. A. Campbell, A. Fert, and O. Jaoul, J. Phys. C **3**, S95 (1970).

[8] O. Jaoul, I. A. Campbell, and A. Fert, J. Magn. Magn. Mater. **5**, 23 (1977).

[9] J. Smit, Physica **17**, 612 (1951).

[10] S. Wakoh and J. Yamashita, J. Phys. Soc. Jpn. **19**, 1342 (1964); J. W. D. Connolly, Phys. Rev. **159**, 415 (1967); C. S. Wang and J. Callaway, Phys. Rev. B **9**, 4897 (1974).

[11] A. V. Gold, J. Appl. Phys. **39**, 768 (1968).

[12] E. M. Pugh, Phys. Rev. **97**, 647 (1955); E. R. Sanford, A. C. Ehrlich, and E. M. Pugh, *ibid.* **123**, 1947 (1961); A. C. Ehrlich, J. A. Dreesen, and E. M. Pugh, *ibid.* **133**, A407 (1964).

[13] L. Hodges, H. Ehrenreich, and N. D. Lang, Phys. Rev. **152**, 505 (1966). See Fig. 1.

[14] C. Herring, in *Magnetism*, edited by G. T. Rado and H. Suhl (Academic, New York, 1966), Vol. 4, pp. 162–164.

[15] J. W. F. Dorleijn and A. R. Miedema, AIP Conf. Proc. **34**, 50 (1976).

[16] L. Berger, P. P. Freitas, J. D. Warner, and J. E. Schmidt, J. Appl. Phys. **64**, 5459 (1988).

[17] H. C. Van Elst, Physica **25**, 708 (1959).

[18] E. N. Mitchell, H. B. Haukaas, H. D. Bale, and J. B. Streeper, J. Appl. Phys. **35**, 2604 (1964).

[19] P. P. Freitas, L. Berger, and J. F. Silvain, J. Appl. Phys. **61**, 4385 (1987).

[20] R. M. Bozorth, Phys. Rev. **70**, 923 (1946).

[21] L. Berger and D. Rivier, Helv. Phys. Acta **35**, 715 (1962).

[22] T. R. McGuire and R. I. Potter, IEEE Trans. Magn. **11**, 1018 (1975).

[23] F. C. Williams and E. N. Mitchell, Jpn. J. Appl. Phys. **7**, 739 (1968).

[24] See a summary of data from five different investigations of γ^{el} in Ni-Fe in Fig. 2 and Ref. 5 of L. Berger, Physica **91B**, 31 (1977).

[25] C. Kittel, *Introduction to Solid State Physics*, 6th ed. (Wiley, New York, 1986), p. 141.

[26] G. A. Burdick, Phys. Rev. **129**, 138 (1963); J. S. Faulkner, H. L. Davis, and H. W. Joy, *ibid.* **161**, 656 (1967).

[27] P. Goy and C. C. Grimes, Phys. Rev. B **7**, 299 (1973).

[28] K. Gilmore, Y. U. Idzerda, and M. D. Stiles, Phys. Rev. Lett. **99**, 027204 (2007).

[29] V. Kambersky, Can. J. Phys. **48**, 2906 (1970).

[30] B. Heinrich, D. Fraitova, and V. Kambersky, Phys. Status Solidi **23**, 501 (1967).

[31] S. Ingvarsson, L. Ritchie, X. Y. Liu, G. Xiao, J. C. Slonczewski, P. L. Trouilloud, and R. H. Koch, Phys. Rev. B **66**, 214416 (2002).

[32] G. Counil, T. Devolder, J. V. Kim, P. Crozat, C. Chappert, S. Zoll, and R. Fournel, IEEE Trans. Magn. **42**, 3323 (2006).

[33] F. A. Ponce, S. M. Bhagat, and P. Lubitz, Solid State Commun. **18**, 521 (1976).

[34] M. H. Seavey and P. E. Tannenwald, J. Appl. Phys. **29**, 292 (1958); F. B. Humphrey, *ibid.* **34**, 1067 (1963).

[35] See Sec. VI of Ref. 5.